RSC Advances

ROYAL SOCIETY OF CHEMISTRY

www.rsc.org/advances

Dynamic Article Links ►

Cite this: DOI: 10.1039/c0xx00000x

www.rsc.org/xxxxxx

PAPER

Polymethacrylic acid–facilitated nanofiber matrix loading Ag nanoparticles for SERS measurements †

Hui Yang,[a] and Cheng Zhi Huang*[a,b]

Received (in XXX, XXX) Xth XXXXXXXXX 20XX, Accepted Xth XXXXXXXXX 20XX

DOI: 10.1039/b000000x

Nanofiber matrix loading Ag nanoparticles have been applied for SERS measurements with the shortcomings of poor reproducibility. By introducing polymethacrylic acid (PMAA) into the electrospun solutions in this contribution, fairly uniform PMAA/poly (N-vinylpyrrolidone) (PVP) ultrafine fibers containing silver nanoparticles (AgNPs) were successfully prepared via electrospun by means of in situ photo reduction of silver ions. PMAA can greatly improves the absorbing amounts of silver ions in the polymer owing to its liner structure with abundant carboxyl, that makes the content and size of formed AgNPs in the polymer matrix could be easily controlled under different light source (desk lamp, 365 nm UV lamp, and 254 nm UV lamp, etc). With the electrospun AgNPs/PMAA/PVP fibrous membranes, Malachite green (MG), a significant environmental organic pollutant for its genotoxicity, was successfully detected with RSD values below 0.2% through SERS signals.

Introduction

Incorporation of functional molecules into the host materials may further improve the comprehensive properties of composites because the "single component" in the host material has a limited number of functions.[1,2] Research on composites materials composed of nanoparticles dispersed within a polymeric matrix has attracted a great deal of attention, since these materials offer tremendous options for combining properties originating from both the inorganic components and the polymers.[3,4] Nanoparticles exhibit unique properties which differ from their bulk materials, owing to the quantum size effects and the large number of unsaturated surface atoms. The introduction of polymeric matrix provides additional qualities, such as the processability, the solubility or the thermal stability of the systems. A wide range of metal nanoparticles have been formed within polymer templates including Ag, Au, Cu, Pt, and Pd.[5-7] In this way, composite materials possessing novel catalytic,[8] conductive,[9] or sensing properties can be obtained.[10-12] Thus, it still remains a worthwhile yet challenging to pursue a better method and explore their novel applications of these composite materials.

At present, most of the methods reported to prepare metal nanoparticles within a polymeric matrix are based on situ reactions by wet-chemistry preparation strategy. That is, the particles are generated from the respective metal precursors in the presence of the matrix polymer. The options range from chemical reductions,[13] photoreductions[14] and decompositions,[15] to thermal process[16] and hydrogen-bonding interaction.[17] Compared with the methods mentioned above, however, electrospinning is a more facile and ingenious method to fabricate polymer-encapsulated metal nanoparticles, by which many kinds of functional nanoparticles such as carbon nanotubes, silver nanoparticles (AgNPs) *etc*. can be incorporated into the polymer. Especially, the addition of AgNPs within polymer nanofiber by electrospinning technique have been attracting intensive scientific interest because elemental silver have been used for decades as surface enhanced Raman scattering (SERS) substrates.[18-21] Thus, the AgNPs/polymer composite nanofiber mat by electrospinning should be particularly well-suited for using as SERS substrates for the following reasons: (1) being suitable for surface modification during sample preparation; (2) exhibiting excellent mechanical resilience; (3) being three-dimensionally porous for analytes to easily access. However, a remaining question is that most of the current procedures for preparing the AgNPs/polymer composite nanofiber mat by electrospinning have significant deficiency such as the complexity, the low yield and the aggregation of AgNPs, which produces poor reproducibility for detection results.

Polymethacrylic acid (PMAA), a common polyelectrolyte, has a strong affinity for silver ions due to its carboxylic acid group, which has also been proven to be a versatile template for the preparation of Ag nanoclusters.[22] Illumination is used as a convenient tool to dynamically manipulate the synthesis and shape transformation of metal nanoparticles. Therefore, in this work, the electrospinning solution comprised of $AgNO_3$, PMAA and PVP was used to fabricate the nanofiber mat by electrospinning technique with the aid of light irradiation, resulting in the AgNPs/polymer composite nanofiber mat (illustrated in scheme 1). The advantages of the present strategy might be: (1) the high yield of AgNPs for introducing the PMAA into electrospun solution; (2) highly monodisperse particles with uniform size and shape due to the dispersing and stabilizing action of polymer media; (3) the ability to control nanoparticle growth with light opening up novel synthesis avenue.

Furthermore, by using the Raman report molecules, crystal violet (CV) and *p*-aminothiophenol (*p*-ATP) as typical examples, it was found that the as-prepared AgNPs/polymer nanofiber mats exhibit very strong SERS activity. The SERS signals display perfect stability under continuous laser radiation as well as good uniform response. We further demonstrate that the AgNPs/polymer nanofiber mats can be conveniently applied as SERS substrate by taking the example of malachite green (MG), a significant environmental organic pollutant for its genotoxicity and carcinogenicity[23] that often illegally used in the aquaculture industry, showing that the SERS substrate can give good reproducible results.

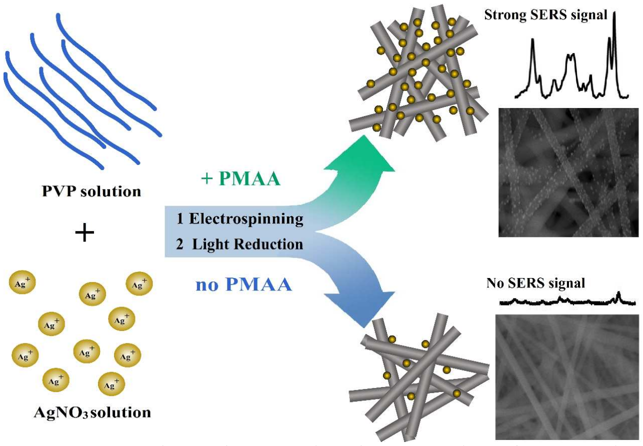

Scheme 1. A scheme demonstrating the preparation of SERS-active electrospun nanofibers surface-decorated with AgNPs.

Experimental Section

Reagents

The polyvinylpyrrolidone (PVP) (Mw=1 300 000), crystal violet (CV) and *p*-aminothiophenol (*p*-ATP) used in this study were purchased from Aladdin, Ltd. Silver nitrate, malachite green (MG), and poly (methacrylic acid) (PMAA) (Mw=9500) and dehydrated alcohol (>99%) was supplied from Sigma-Aldrich and Chongqing Chuandong Ltd., respectively. All chemicals were used without further purification. Water was purified by a Milli-Q system (Millipore).

Apparatus

Desk lamp (11 W), 365 nm UV lamp and 254 nm UV lamp with the power of 11 W were employed as the irradiation sources. An S-4800 scanning electron microscope (SEM, Hitachi, Tokyo, Japan) and transmission electron microscopy (TEM, Hitachi) were used for SEM, and TEM imaging, respectively. X-ray photoelectron spectroscopy (XPS) analysis was performed on an ESCRLRB250X (America) cispectrometer with a standard Al K source (hν=1486.6 eV). X-ray powder diffraction (XRD) patterns were obtained by a Shimadzu XRD-7000 (Beijing Purkinje General Instrument Co. Ltd.) and filtered Cu-Kα (1.5405 Å) radiation source under the operating voltage and current of 40 kV and 50 mA. UV-Vis absorption spectra were measured at room temperature with a Hitachi U-3600 spectrophotometer (Shimadzu, Japan). Fourier Transform Infrared (FT-IR) spectra were recorded by a Fourier transform infrared Spectrometer (Shimadzu, 8400S, Japan) from 4000 to 500 cm^{-1} at room temperature. The prepared electrospun mats were dried overnight at 30 ˚C under vacuum. For the measurement of SERS spectra, a LabRAM-HR Raman spectrometer (HORIBA Jobin Yvon, France) was used and the excitation source was 532 nm using an accumulation time of 1 s.

Preparation of electrospun solution

PVP powders were first dissolved in ethanol to make an 8 wt% solution. A certain amount of freshly prepared solution of silver nitrate was made by dissolving in water and transferred to the PVP solution. The $AgNO_3$/PVP mixed solution was magnetically stirred for 3 h. A known amount of 10 wt% PMAA was added to the $AgNO_3$/PVP mixed solution. The relative concentrations of the solutions are denoted as a percentage value, for instance, a 200% silver/MAA molar ratio means that there are two Ag ions per methacylic acid unit. The above mixture was magnetically stirred until PMAA was dispersed completely to form the electrospun solution. For comparison, the electrospun solution containing $AgNO_3$ only without PMAA was prepared similar to the above method.

Electrospinning

The electrospinning solution was then filled in a 10 mL tip plastic syringe. The electrospun nanofibers were prepared with commercial electrospinning equipment (DNF-001, Beijing Kaiweixin Technology Co., Ltd, China). The electrospinning parameters were set at an applied voltage of 20 kV, a collection distance of 20 cm, and the electrospinning solution feed rate controlled at 0.03 mm/min. The sample nanofibers were collected as overlaid membranes on electrically grounded aluminum foil that covered the plate. After being electrospun, the formed electrospun fibrous mats were vacuum dried at 30 ˚C overnight to remove the residual solvent and moisture for characterizations.

Photo-reduction

The as-prepared fibrous mats were placed in a dark room and were subjected to light for a certain time. With irradiation time the mats gradually changed from white to light pink or to dark pink or to khaki, which depended on the different light source if exposure time were long enough. Three different sources of light were used to produce the AgNPs including desk lamp and UV light with different wavenumber, namely, 365 nm and 254 nm. When using the desk lamp the experiments were performed in a dark cupboard to avoid other kind of light. Different sources lead to different results.

Reproducibility detection with the SERS matrix

The obtained electrospun mats were immersed into 10^{-4} M *p*-ATP ethanol solution overnight firstly. Then the mats were washed thoroughly with ethanol to remove unbound *p*-ATP molecules and finally the samples were dried at room temperature to evaporate all of the ethanol. 10^{-6} M CV and MG aqueous solution were used by following the same treatment as above mentioned. Local fishery water as a comparison was also employed by filtering with 0.45 μm filter film after boiling to expel the impurities and then stored at room temperature.

Results and Discussion

Preparation of electrospun AgNPs/PMAA/PVP mats

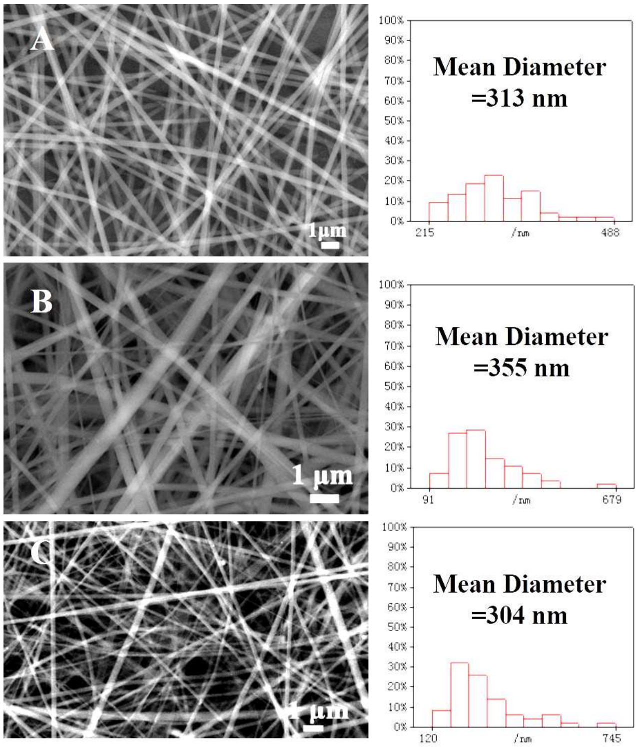

Fig. 1 SEM images and diameter histograms of electrospun nanofibers (A) PVP only, (B) PMAA/PVP, and (C) $AgNO_3$/PMAA/PVP before illuminated, respectively.

Under the optimal electrospinning parameters, smooth and uniform PVP, PMAA/PVP, and $AgNO_3$/PMAA/PVP nanofibers before illuminating were prepared at first. Fig. 1 showed SEM images of the composite nanofibers, and the size distribution histograms of nanofibers that calculated from the corresponding SEM images, giving a mean diameter of 313 nm, 355 nm, and 304 nm, respectively.

Then, photo-reduction treatment was introduced under different light source for 24 h. Typical SEM images of AgNPs/PMAA/PVP nanofiber fabricated with different light source are showed in Fig. 2. As it can be seen, the hybrid nanofibers exhibited a smooth surface and uniform diameter.

After the formation of AgNPs, no apparent change was observed either in the size or the overall pattern of the AgNPs/PMAA/PVP composite nanofibers. Moreover, the mean diameter of AgNPs/PMAA/PVP nanofibers at any light source was apparently smaller than that of PVP or PMAA/PVP nanofibers without AgNPs, suggesting that the addition of $AgNO_3$ changed the conductivity, surface tension and viscosity of the electrospining solution, resulting in the changeable of the diameter. It was interesting that abundant AgNPs on the surface of PMAA/PVP at both desk lamp and 365 nm UV lamp could be observed, but rare AgNPs can be at the 254 nm UV lamp, we suppose it's the energy of light source that might be responsible for the reductive efficacy of hybrid nanofibers.

From Fig. 2 inset, it could be clearly seen that the AgNPs were distributed on the nanofiber surface with a high density under the condition of desk lamp and 365 nm UV lamp, which was great for the improvement of sensing performance. The TEM images clearly showed that both the inner and outer surface distributed large amount of AgNPs with the diameter rang from 5 to 19 nm. The TEM image also indicated that there was no change to the nanofibers' morphology during the reduction of the silver ions.

Characterization of electrospun AgNPs/PMAA/PVP mats

The effects of the light source and the photo-reduction time on the formation of AgNPs were also examined. The light source contained desk lamp, 365 nm UV lamp, and 254 nm UV lamp and the photo-reduction time ranged from 0 h to 24 h. The corresponding changeable photographs (Fig. 3) and SEM images showed the reductive process (SI, Fig. S1). Silver ion has a strong optical properties in a certain visible light region, silver ions can be converted into silver atoms induced by ultraviolet light, further reunion into the form of nanoparticles.[24] Herein, the photochemical reaction of generating AgNPs as depicted in the following chemical equation:

$$2Ag^{+} + 2NO_3^{-} \xrightarrow{h\nu} 2Ag^{0} + 2NO_2 + O_2 \qquad mAg^{0} \xrightarrow{h\nu} (Ag)_m$$

As a result, the treatment of irradiation played a major role in forming AgNPs embedded in the nanofibers. The amounts of AgNPs on the polymer increase as the illuminated time increase for the same light source. Presumably, this is because of slower diffusion of reactive species produced by light source penetrate into the interior of the thicker chain length polymers.

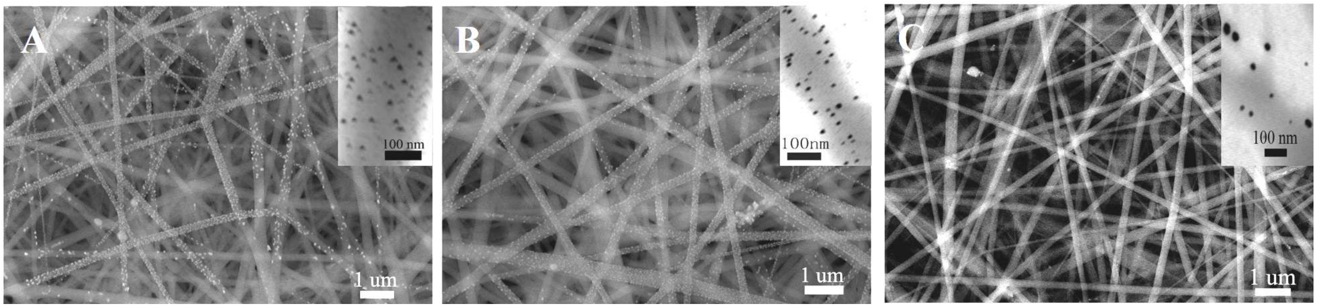

Fig. 2 Morphology of the electrospun fiber mats from the $AgNO_3$/PMAA/PVP solution that had been illuminated by different light sources for 24 h. (a) desk lamp, (b) 365 nm UV lamp, (c) 254 nm UV lamp, and the inset is the TEM image of AgNPs/PMAA/PVP respectively.

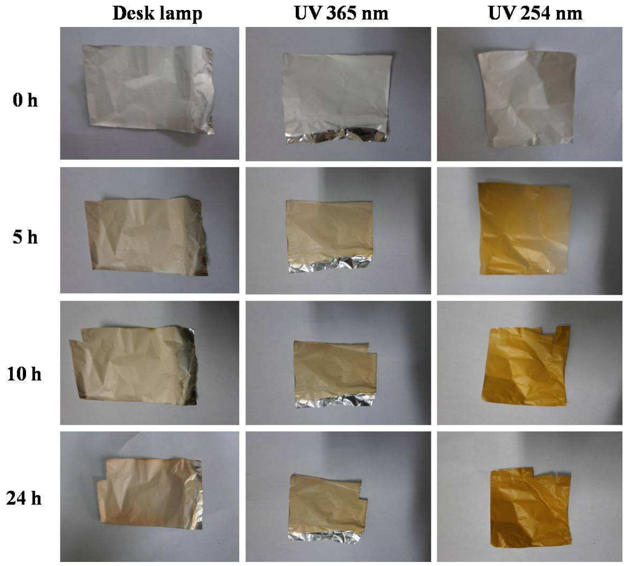

Fig. 3 Photographs of electrospun fiber mats from the $AgNO_3$/PMAA/PVP solution that had been illuminated by different light sources for different illuminated time.

More detailed information regarding the chemical and bonding environment of the PMAA/PVP and AgNPs were ascertained using X-ray photoelectron spectroscopy (XPS). Fig. 4A showed the fully scanned spectra, demonstrating that C, O, N and Ag existed in AgNPs/PMAA/PVP. It can be seen from the inset that the peaks occurred at 368.3 eV and 374.3 eV, which well corresponds to Ag $3d_{5/2}$ and $3d_{3/2}$ binding energy, respectively. The splitting of the 3d doublet is 6 eV, indicating the metallic nature of silver.[25] XPS spectra of the C 1s, O 1s and N 1s of PVP were not changed after AgNPs were immobilized into PMAA/PVP. Moreover, there was no carboxyl carbon (O-C=O) peak which was located at 289 eV, suggesting that the carboxyl of PMAA not coordinate with Ag ions but adsorb large amount Ag ions. According to the XPS spectra, it was concluded that carbonyl oxygen of PVP donated lone pair electrons to sp orbitals of silver, which decreased the electron density of carbonyl oxygen and increased the electron density of silver. Thus, it was the strong Ag: O coordination that prevented the Ag ions immobilized in PMAA/PVP nanofibers from agglomeration. Moreover, the steric effect of PVP might also help to forbid silver grain growth. More importantly, PMAA is not only acting as an effective stabilizer that prevents agglomeration of the AgNPs, but it is also essential for well morphologies of nanofibers formation when used in the appropriate concentration.

In order to further determine the crystal nature of AgNPs, the crystallinity of AgNPs immobilized into the PMAA/PVP nanofibers was also analyzed using X-ray diffraction (XRD) (Fig.4B). A typical XRD pattern of as-prepared AgNPs showed the diffraction peaks with 2θ values of 38.2°, 44.2°，64.4° and 77.4°,which were respectively corresponding to the (111), (200), (220) and (311) (specific for elemental Ag were present) crystal faces of the face-centered cubic (*fcc*) structure of metallic silver, in agreement with the literature,[26, 27] which further supported that the AgNPs were successfully reduced on the PMAA/PVP polymer matrix.

The FTIR spectra (Fig. 4C) of PMAA/PVP nanofibrous mats displays a significant difference before and after immobilization of AgNPs. A strong absorption peak at 1648 cm^{-1} assigned to the free carbonyl group (C=O asymmetric stretching) of PVP and the peak at 1656 cm^{-1} attributed to COO- asymmetric vibrations of PMAA. A new peak at 1391 cm^{-1} appeared after AgNPs loaded indicated the interaction between AgNPs and carbonyl groups of PVP. Moreover, after the formation of AgNPs in the PMAA/PVP nanofibers, the spectral features of the nanofibers seemed to be broader.

Further investigation found that the size of AgNPs on the surface of PMAA/PVP nanofibers could be controlled by appropriately adjusting the light source during the *in situ* reduction. It is well-known that the optical absorption spectra of noble metal NPs are dominated by their sizes and shape.[28] Therefore, the UV-Vis absorption spectra of the as-prepared AgNPs/PMAA/PVP composites were carried out, and the corresponding results were shown in Fig. 4D. There were no distinct adsorption peaks for the $AgNO_3$/PMAA/PVP before illuminated in the visible region. Nevertheless, a relatively strong adsorption peak centered at around 430 nm was observed after illuminated (Fig. 4D (2)) due to the Surface Plasmon Resonance (SPR) absorption of AgNPs. The inset of Fig. 4D showed the optical images of the as-prepared products dissolved in water. The $AgNO_3$/PMAA/PVP before illuminated were colorless, indicating that PMAA did not have an effect on the optical properties of AgNPs/PMAA/PVP. And, the AgNPs/PMAA/PVP composites after reduction were brown-yellow in accordance with its absorption peak.

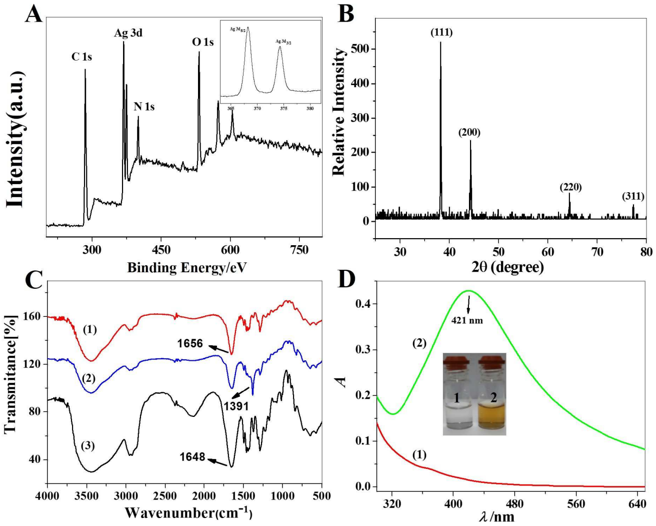

Fig. 4 (A) XPS fully scanned spectra of the sample AgNPs/PMAA/PVP, the insert is the XPS spectra of Ag 3d. (B) X-Ray diffraction pattern of AgNPs immobilized into the PMAA/PVP nanofibers. (C) FTIR spectra of PMAA/PVP nanofibrous mats before and after the immobilization of AgNPs. (1) PMAA/PVP mat, (2) AgNPs/PMAA/PVP mat, and (3) PVP mat, respectively. (D) UV-vis absorption spectra of aqueous suspensions of as-prepared products; the insert is the optical images of as-prepared products in reaction solution: (1) $AgNO_3$/PMAA/PVP before illuminated; (2) $AgNO_3$/PMAA/PVP after 365 nm UV lamp illuminated.

Role of PMAA in the AgNPs/PMAA/PVP system

Role of PMAA in the AgNPs/PMAA/PVP system

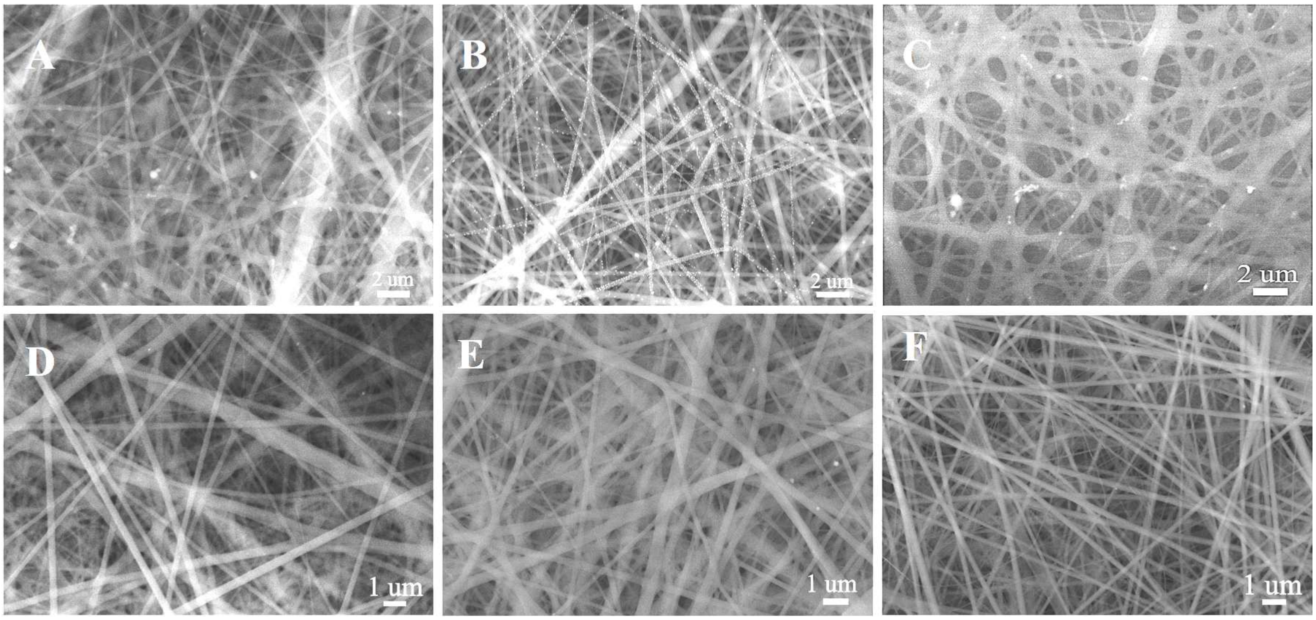

Fig. 5 SEM images of electrospun fiber mats from the $AgNO_3$/PMAA/PVP solution with different ratios of Ag: MAA after illuminated by 365 nm UV lamp (A) Ag^+: MAA=200:1, (B) Ag^+: MAA=400:1, and (C) Ag^+: MAA=600:1, respectively. SEM images of electrospun fiber mats from the $AgNO_3$/PVP solution without PMAA after illuminated by different light source for 24 h (D) desk lamp, (E) 365 nm UV lamp, and (F) 254 nm UV lamp, respectively.

In order to gain insight into the positive effect of the PMAA, the SEM images were investigated. The concentration of PMAA in the precursor solution was varied (Fig. 5A-C). Bead-free fibers were obtained at any content of PMAA. From figure 5A-C, it was apparently limited AgNPs were formed on the surface of PVP at the molar ratio of 200:1 (Ag: MAA). The fibers morphology became dramatically cross-linking with the increasing concentration to 600:1 (Ag: MAA) due to the difficult to phase separation. When the molar ratio was 400:1, the $AgNO_3$/PMAA/PVP system can be tuned to facilitate electrospinnability by a proper formulation of the dispersion and thus plurinatality, uniform distribution, and high performance AgNPs/PMAA/PVP composites were obtained. In contrast to the case of without PMAA, SEM images (Fig. 5D-F) of electrospun fiber mats from only the $AgNO_3$/PVP solution, nearly no AgNPs were observed. This result indicated the importance of PMAA introduced in this system.

Because the PMAA chain can provide adsorptive –COOH groups on the polymer nanofibers, it can serve as carriers for silver ions to make as more silver ions as possible to absorb on the surface of polymer. Naturally, a distinctive feature is the high yield and uniform distribution of AgNPs on the surface of polymer. Overall, with the adsorption of PMAA and the high coordination affinity for silver ions of PVP, we present an easily controlled preparation of AgNPs/polymer composites using PMAA because of itself is a linear molecule, as the adsorbing agent to absorb large amounts of silver ions, meanwhile, the polymer PVP as the stabilizer to protect the AgNPs. The polymer template usually serves to both control particle size and passivates the surface of the nanoparticles against agglomeration.

SERS properties of electrospun AgNPs/PMAA/PVP mats

The formed AgNPs in PMAA/PVP fibers had high local electromagnetism, and they could be used as SERS substrates for molecular sensing with high sensitivity and universality.

To estimate the SERS activity of the AgNPs/PMAA/PVP, 10^{-4} M of *p*-aminothiophenol (*p*-ATP) aqueous solution was chosen as the probe molecule because *p*-ATP has distinct Raman features and it is easy to absorb on the surface of AgNPs for the bond of –SH (obtained SERS spectra are shown in Fig. 6A). The SERS spectra of *p*-ATP on the nanofibrous mats that before illuminated were also collected as the contrast. Additionally, the AgNPs/PMAA/PVP nanofiber mats after being immersed in *p*-ATP ethanol solution so that *p*-ATP molecules can permeate into the fiber, access the AgNPs, and be trapped in the hot spot region in an ethanol solution. The primary vibrations of *p*-ATP were confirmed according to the literature.[29] Two sets of bands were observed on the SERS spectra of *p*-ATP on the as-prepared substrates: 1580, 1187, and 1082 cm^{-1} assigned to a1 vibration modes and 1436, 1388, and 1147 cm^{-1} assigned to the b2 vibration modes. The relative intensity of the peaks in the spectra on AgNPs/PMAA/PVP indicated that the *p*-ATP adsorbed on AgNPs according to the cleavage of the Ag-S bond in the same orientation. It was distinct that the intensity of SERS spectra on AgNPs/PMAA/PVP by 365 nm UV lamp and desk lamp were much stronger than that by 254 nm UV lamp. A possible reason was proposed to explain the difference of the intensity: the content of adsorpted *p*-ATP on AgNPs are different, it is obviously that the amounts of AgNPs by 365 nm UV lamp and desk lamp illuminated are more than that by 254 nm UV lamp, which corresponding to the results of the SEM images. The more AgNPs, may be some aggregated AgNPs, the stronger SERS enhancement due to the more AgNPs on the nanofibers, the more *p*-ATP molecules were adsorbed and the hot spots formed in the nanoscale junctions and interstices.

To further investigate the universality of the as-prepared substrates, in addition to *p*-ATP, crystal violet (CV) was also used as probe molecules. Fig. 6B presented the SERS spectra of 10^{-6} M CV on the AgNPs/PMAA/PVP substrates with different light sources. The characteristic SERS peaks of CV molecules can be identified and their intensities also dramatically change with different light source. Maximum enhancement occurred at light sources by desk lamp and 365 nm UV lamp. As can be seen in Fig. 6B, the SERS band at 806 cm^{-1}, 914 cm^{-1}, 1177 cm^{-1}, 1370 cm^{-1}, and 1625 cm^{-1} assigned to the characteristic peaks for CV molecules. It means that in the focal area there is rather small number of highly SERS-active sites, which, provide very high surface enhancement.

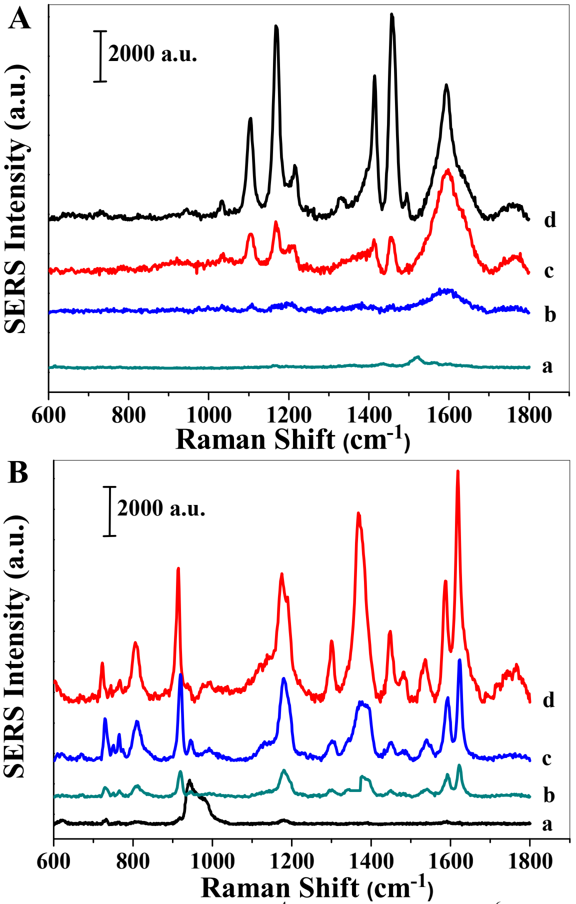

Fig.6 Typical SERS spectra of 10^{-4} M *p*-ATP (A) and 10^{-6} M CV (B) solutions on (a) AgNPs/ PMAA/PVP before illuminated, (b) 254 nm UV lamp, (c) desk lamp, and (d) 365 nm UV lamp AgNPs/PMAA/PVP nanofibrous mats, respectively.

To use SERS as a routine analytical tool, the reproducibility of Raman signals is of crucial importance, and is estimated by the relative standard deviation (RSD) of a major SERS peak. In this work, we collected SERS spectra of CV molecules with a concentration of 10^{-6} M from thirteen randomly selected positions estimate on the AgNPs/PMAA/PVP electrospun nanofiber mats, and the RSD were calculated by the method reported.[30] With this method, both an overall impression and a detailed depiction of reproducibility can be provided (Fig. S2). In this case, RSD values of signal intensities of major SERS peaks were observed to be below 0.2%, revealing a good reproducibility across the entire area of the optimized AgNPs/PMAA/PVP electrospun mats (Table S1).

According to the results of *p*-ATP and CV SERS spectra, it was evident that, with the enrichment from the PMAA, the SERS intensity of the probe molecules on AgNPs/PMAA/PVP was stronger than that on AgNPs/PVP, which enables qualitative detection of *p*-ATP and CV. As compared to the common AgNPs/polymer composites, the AgNPs reported previously were mostly encapsulated in polymer matrixes, thus, the molecules of analytes applied to SERS have to diffuse/permeate into nanofibers to access these AgNPs. In this study, AgNPs that attached to electrospun nanofibers can adsorb analytes directly on their surfaces, leading to superior SERS sensitivity. The high density AgNPs are attributed to the three-dimensional network nanostructure of the AgNPs/PMAA/PVP membrane, which provide large surface area-to-volume ratio. Most importantly, PMAA serve as the carrier of silver ions. SEM images that without PMAA analysis indicates that the apparent lower density AgNPs on the surface of PVP nanofibers. It is known that the high probe density can facilitate the improvement of sensitivity by maximizing the number of target molecules captured by the sensing material. The result further demonstrates the superior of the composite as SERS substrates.

AgNPs/PMAA/PVP nanofiber mats as SERS substrates for MG detection

Malachite green (MG) is a cationic triphenylmethane dye used in the aquaculture industry and is banned in several countries for its genotoxicity and carcinogenicity.[23] Currently, various analytical methods, including liquid chromatography,[31] electrochemistry,[32] connection of chromatography and mass spectrometry,[33,34] capillary electrophoresis have been employed.[35] However, they are restricted by poor detection limit, time consuming and indirect measurements. Therefore, the development of highly sensitive and selective analytical methodology of MG is of great importance. SERS is a rapid and sensitive analytical method in various areas,[36,37] as a result, the SERS signals was applied to the quantitative analysis of MG in this work.

Due to the π electron of the benzene ring and the positive charge of MG, MG can be integrated with the pyrrole ring of PVP and PMAA well through π-π stacking and electrostatic interaction. Taking the advantages of the chemical enhancement effect from PVP and the electromagnetic enhancement effect from PMAA, MG can be detected sensitively by using the AgNPs/PMAA/PVP composite nanofibers as SERS substrates. Fig. 8A displays the SERS spectra of 2×10^{-6} M MG on the AgNPs/PMAA/PVP substrates with different light sources. As can be seen, a strong SERS spectrum was achieved with the UV light 365 nm. The most prominent peaks at 1175, 1367 and 1618 cm^{-1} was assigned to the in-plane modes of C-H bending, N-phenyl stretching, and C-C stretching, respectively. The peak around 917, 1219, 1398 cm^{-1} were attributed to C-H out-of-plane bending, C-H rocking and N-phenyl stretching. However, the SERS intensities of the MG reduced by UV light 254 nm and desk lamp were lower than that UV light 365 nm.

Under the optimal light source, SERS spectra of different concentration of MG were detected as shown in Fig. 7B. It can be seen that the intensity of the SERS spectra increased with the increasing concentrations of MG. The SERS intensity of the vibration located at 1618 cm^{-1} *vs.* the concentration of MG was also plotted in Fig. 7B, which revealed a good linearity over MG concentration range from 0.5 μmol/L to 100 μmol/L of MG (r^2=0.9929), and the equation of liner regression was I=1135.2+80.5c (MG, 10^{-6} mol/L). Considering that the as-prepared nano-hybrids have a high enhancement effect, they can be used as a potential SERS sensor to detect environmentally harmful substances.

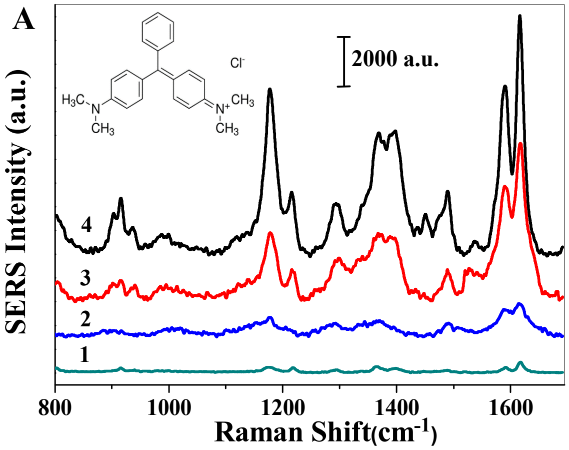

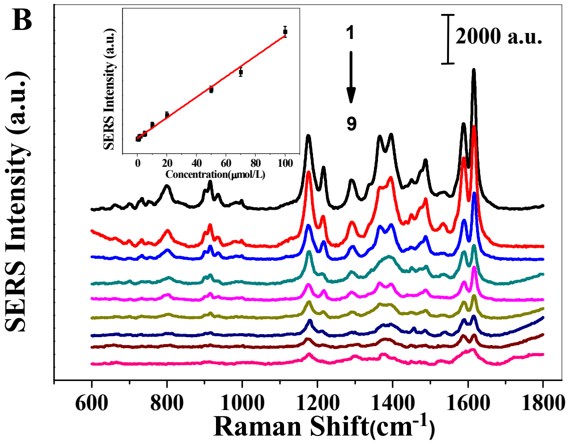

Fig. 7 (A) SERS spectra of 2 μmol/L MG on (1) $AgNO_3$/PMAA/PVP nanofibrous mats before illuminated, (2) illuminated by 254 nm UV lamp, (3) desk lamp, and (4) 365 nm UV lamp, respectively. (B) SERS spectra of different concentrations of MG in water: 1-9: 100, 70, 50, 20, 10, 5, 2, 1, 0.5 μmol/L. All of the electrospun membranes were reduced by UV light 365 nm. Laser wavelength: 532 nm; power: 28 mW; lens: 50×objective; acquisition time: 1 s.

To investigate its application in practical sample analysis, the proposed procedure was performed to detect MG in a fishery water sample and the studies of recovery were carried out on samples. An additional procedure to remove the environmental pollutants was unnecessary. It was found that the recoveries of these samples are between 94-102.5% (Table S2). The real sample determination proved that the AgNPs/PMAA/PVP composite nanofibers are efficiently SERS substrates for detection of MG in water samples, and the ignorance of background indicates the potential application to detect MG in other practical systems.

Conclusions

In summary, we developed a convenient and cost-effective approach to fabricate the PMAA/AgNPs/PVP composite mats with well-dispersed AgNPs on the electropun nanofibers. Based on this novel composite, the highly active SERS substrates for exhibiting high performance, good stability, as well as dramatic capability of repetitive measurement were constructed. The density of AgNPs, which had important impact on SERS activity, could be controlled by different light source and illuminate time. The introduction of PMAA in the AgNPs/PMAA/PVP composites plays an important role on the electrospun nanofibrous mats because it adsorbs large amount of silver ions into the polymer. The novelty of the methodology provides a universal platform for the fabrication of composite membranes by decorating noble metal nanoparticles on electrospun nanofibers, which could possibly be used widely in a broad range of applications.

Acknowledgements

This work was financially supported by the Natural Science Foundation of China (21035005) and the Cultivation Plan of Chongqing Science & Technology Commission for 100 Outstanding Science and Technology Leading Talents.

Notes and references

[a] *Key Laboratory of Luminescence and Real-Time Analytical Chemistry (Southwest University), Ministry of Education, College of Chemistry and Chemical Engineering, Southwest University, Chongqing 400715, China. E-mail: chengzhi@swu.edu.cn, Tel: (+86) 23 68254659, Fax: (+86) 23 68367257.*

[b] *College of Pharmaceutical Science, Southwest University, Chongqing 400716, China*

† Electronic Supplementary Information (ESI) available: Experimental section and additional figures (Fig. S1-S2) and table （Table S1-S2）. See DOI: 10.1039/b000000x/

1 R. Ostermann, J. Cravillon, C. Weidmann, M. Wiebcke and B. M. Smarsly, *Chem. Commun.*, 2011, **47**, 442-444.
2 H. Yang, P. F. Gao, W. B. Wu, X. X. Yang, Q. L. Zeng, C. Li and C. Z. Huang, *Polym. Chem.*, 2014, **5** , 1965-1975.
3 Davies S C and Klabunde K J, *Chem. Rev.*, 1982, **82**, 153-208.
4 R. M. Crooks, M. Zhao, L. Sun, V. Chechik and L. Yeung, *Accounts Chem. Res.*, 2001, **34**, 181-190.
5 J. Song, M. Chen, M. B. Olesen, C. Wang, R. Havelund, Q. Li, E. Xie, R. Yang, P. Bøggild, C. Wang, F. Besenbacher and M. Dong, *Nanoscale*, 2011, **3**, 4966-4971.
6 K. Gries, H. Vieker, A. Gölzhäuser, S. Agarwal and Andreas Greiner, *Small*, 2012**, 8**, 1436-1441.
7 W. Wang, Z. Feng, W. Jiang and J. Zhan, *CrystEngComm*, 2013, **15**, 1339-1344.
8 P. Zhang, C. Shao, Z. Zhang, M. Zhang, J. Mu, Z. Guo and Y. Liu, *Nanoscale*, 2011, **3**, 3357-3363.
9 J. Mu, C. Shao, Z. Guo, Z. Zhang, M. Zhang, P. Zhang, B. Chen and Y. Liu, *ACS Appl. Mater. Interfaces*, 2011, **3**, 590-596.
10 Z. Zhang, C. Shao, Y. Sun, J. Mu, M. Zhang, P. Zhang, Z. Guo, P. Liang, C. Wang and Y. Liu, *J. Mater. Chem.*, 2012, **22**, 1387-1395.
11 H. Wang, D. Wang, Z. Peng, W. Tang, N. Li and F. Liu, *Chem. Commun.*, 2013, **49**, 5568-5570.

12 D.He, Bo Hu, Q. F. Yao, K. Wang and S. H. Yu, *ACS nano*, 2009, **3**, 3993-4002.

13 S. Xiao, W. Xu, H. Ma and X. Fang, *RSC Adv.* 2012, **2**, 319-327.

14 Z. Y. Li, H. M. Huang, T. C. Shang, F. Yang, W. Zheng, C. Wang and S. K. Manohar, *Nanotechnology*, 2006, **17**, 917-920.

15 H. He, W. P. Cai, Y. X. Lin and Z. F. Dai, *Langmuir*, 2011, **27**, 1551-1555.

16 A. C. Patel, S. Li, C. Wang, W. Zhang and Y. Wei, *Chem. Mater.*, 2007, **19**, 1231-1238.

17 H. Dong, D. Wang, G. Sun and J. P. Hinestroza, *Chem. Mater.*, 2008, **20**, 6627-6632.

18 C. H. Lee, L. M. Tian, A. Abbas, R. Kattumenu and S. Singamanen, *Nanotechnology*, 2011, **22**, 275311-275318.

19 C. L. Zhang, K. P. Lv, H. P. Cong and S. H. Yu, *Small*, 2012, **8**, 648-653.

20 C. L. Zhang, K. P. Lv, H. T. Huang, H. P. Cong and S. H. Yu, *Nanoscale*, 2012, **4**, 5348-5355.

21 W. Y. Zhang, X. Z. Xiao, C. Lv, J. Zhao, G. Wang, X. Gu, R. Zhang, B. B. Xu, D. D. Zhang, A. W. Li, Y. L. Zhang and H. B. Sun, *Macromolecular Res.*, 2013, **21**, 306-310.

22 H. X. Xu and K. S. Suslick, *ACS nano*, 2010, **4**, 3209-3214.

23 D. J. Alderman, *J. Fish Dis.*, 1985, **8**, 289-98.

24 P. Rujitanaroj, N. Pimpha, P. Supaphol. *J. Appl. Polym. Sci.*, 2010, **116**, 1967-1976.

25 D. Lin, H. Wu, R. Zhang and W. Pan, *Chem. Mater.*, 2009, **21**, 3479-3484.

26 D. Cheng, X. Zhou, H. Xia and H. S. O. Chan, *Chem. Mater.*, 2005, **17**, 3578-3581.

27 Y. Lu, Y. Mei, M. Schrinner, M. Ballauff, M. W. Moller and J. Breu, *J. Phys. Chem. C*, 2007, **111**, 7676-7681.

28 B. Chen, X. Jiao and D. Chen, *Cryst. Growth Des.*, 2010, **10**, 3378-3386.

29 M. Osawa, N. Matsuda, K. Yoshii and I. Uchida, *J. Phys. Chem.*, 1994, **98**,12702-21707.

30 B. Zhang, H. Wang, L. Lu, K. Ai, G. Zhang and X. Cheng, *Adv. Funct. Mater.*, 2008, 1**8**, 2348-2355.

31 K. Mitrowska, A. Posyniak and J. Zmudzki, *J. Chromatogr. A*, 2005, **1089**, 187-192.

32 P. Ngamukot, T. Charoenraks, O Chailapakul, S. Motomizu and S. Chuanuwatanakul, *Anal. Sci.*, 2006, **22**, 111-116.

33 L. Valle, C. D´ıaz, A. L. Zanocco and P. Richter, *J. Chromatogr. A*, 2005, **1067**, 101-105.

34 P. Scherpenisse and A. A. Bergwerff, *Anal. Chim. Acta*, 2005, **529**, 173-177.

35 A. A. Bergwerff and P. Scherpenisse, *J. Chromatogr. B*, 2003, **788**, 351-359.

36 W. L. Fu, S. J. Zhen and C. Z. Huang, *Analyst*, 2013, **138**, 3075-3081.

37 S. Lee, J. Choi, L. Chen, B. Park, J. B. Kyong, G. H. Seong, J. Choo, Y. Lee, K. H. Shin, E. K. Lee, S. W. Joo, K. H. Lee, *Anal. Chim. Acta*, 2007, **590**, 139-144.